Systems & Control Letters 167 (2022) 105323

Contents lists available at ScienceDirect

Systems & Control Letters

journal homepage: www.elsevier.com/locate/sysconle

Observer design for multivariable transport-reaction systems based on spatially distributed measurements

Ivan F.Y. Tello [a,b,c,*], Alain Vande Wouwer [a], Daniel Coutinho [b]

[a] Systems, Estimation, Control, and Optimization (SECO), University of Mons, Belgium
[b] Postgraduate Program in Engineering of Automation and Systems, Federal University of Santa Catarina, Brazil
[c] Department of Electronics, Power Electrical and Mechatronics Engineering, Campus ATE, Technological University of Peru, Peru

ARTICLE INFO

Article history:
Received 13 September 2021
Received in revised form 5 June 2022
Accepted 5 July 2022
Available online 21 July 2022

Keywords:
Distributed parameter systems
State estimation
Linear matrix inequalities
Sum of squares

ABSTRACT

This paper is concerned with the design of observers for a class of one-dimensional multi-state transport-reaction systems considering distributed in-domain measurements over the spatial domain. A design based on the Lyapunov method is proposed for the stabilization of the estimation error dynamics. The approach uses positive definite matrices to parameterize a class of Lyapunov functionals that are positive in the Lebesgue space of integrable square functions. Thus, the stability conditions can be expressed as a set of LMI constraints which can be solved numerically using sum of squares (SOS) and standard semi-definite programming (SDP) tools. In order to evaluate the proposed methodology, a state observer is designed to estimate the variables of a nonisothermal tubular reactor model. Numerical simulations are presented to demonstrate the potentials of the proposed observer.

1. Introduction

Many transport-reaction processes are inherently distributed in space and can be represented by semi-linear partial differential equations (PDEs) with mixed or homogeneous boundary conditions arising from conservation laws as well as mass and energy balances. Examples include thermal processes, biochemical reactors, population and epidemics models [1–3].

On-line state estimation of multivariable transport-reaction systems is a delicate problem in view of the system dimensionality and the fact that providing a comprehensive set of sensors is either physically impossible or too costly. In such a case, the internal states have to be estimated on the basis of the mathematical model and (available) online measurements provided by (usually pointwise) sensors located at strategic positions in the spatial domain [4].

For the purpose of observer design for systems described by partial differential equations (PDEs), the late-lumping approach keeps the distributed nature of the system model and finite-dimensional approximation (if needed) is applied only at the implementation stage. This approach theoretically leads to state estimators with a better performance, since no approximation of the model is made. Nevertheless, it requires the manipulation of more sophisticated mathematical tools and methodologies. The most popular methods for the synthesis of observers using the late-lumping approach are based on semigroup-theory [5,6], backstepping techniques [7–9], and sliding modes [10,11]. Alternatively, it is possible to use a Lyapunov-based synthesis in which the convergence of the observer is ensured by means of exponential stability conditions that can be expressed in terms of linear matrix inequality (LMI) constraints. Thus, the observer design problem is parsed into an SDP formulation which can be solved by LMI solvers such as SeDuMi [12]. This approach has been applied to the design of boundary observers for quasi-linear first order hyperbolic systems [13], H_∞ static observer-based boundary control [14] as well as the observer design for a class of scalar semilinear PDEs [15,16]. Recently, Sum-of-Squares (SOS) optimization methods have been applied to the parametrization of Lyapunov functions as positive functionals using SOS polynomials [17–19], which make the observer design problem convex. It should be emphasized that algorithms for solving SOS programs are fully automated in MATLAB through SOSTOOLS [20]. In this framework, Gahlawat and Peet [18] designed observer-based controllers for a class of scalar linear parabolic PDEs based on boundary measurements. While these previous works have proven remarkably effective, they mostly address linear single-state distributed parameter systems (DPSs) with boundary state measurements. A more general framework is therefore missing for multi-state processes with various in-domain pointwise measurements.

In this context, the contribution of this work is a computationally tractable method for the design of nonlinear Luenberger-like

* Corresponding author at: Systems, Estimation, Control, and Optimization (SECO), University of Mons, Belgium.
E-mail addresses: ivanfrancisco.yupanquitello@umons.ac.be (I.F.Y. Tello), alain.vandewouwer@umons.ac.be (A. Vande Wouwer), daniel.coutinho@ufsc.br (D. Coutinho).

https://doi.org/10.1016/j.sysconle.2022.105323
0167-6911/

observer for a class of multi-state transport-reaction systems having spatially distributed measurements. This method provides a guaranteed estimation error decay rate and is formulated in terms of LMI constraints and a polynomial parametrization in such a way that the corresponding solution provides a convergent estimator. Stability analysis of multi-state processes sets a challenging problem with regard to the derivation of possibly not too conservative conditions to be solved by semidefinite programming (SDP) tools. The proposed methodology uses integration by parts as a fundamental tool as well as the Wirtinger's inequality and the S-procedure for local stability analysis based on sector conditions. With regard to previous works on this subject [21,22], our contribution concerns semilinear multi-state systems with in-domain distributed measurements and sets a less conservative solution by making use of weighted Lyapunov functionals based on SOS and polynomial parametrization. This procedure is inspired by studies that address stability analysis of coupled linear PDE systems [23] and output feedback boundary control of single-state linear PDE systems [18]. It should be noticed that the methodology to be presented concerns a large class of semilinear PDE systems within which the state estimation of distributed biochemical processes is only a particular case.

The reminder of this paper is organized as follows. In Section 2, the system description along with some preliminary assumptions is introduced in order to ensure the well-posedness of the observer design problem. Section 3 introduces the proposed observer synthesis based on the abstract formulation of the error dynamics and the set-up of the sector condition related to the nonlinearity embedded into its dynamics. The main results of this paper, i.e., the LMI formulation of the distributed observation problem, with local exponential stability of the estimation error for pointwise measurement and piecewise measurement, are given in Section 4. Section 5 proposes a numerical application of the proposed observer design to the estimation of the weight fractions of the reactants in a tubular cracking reactor model. Section 6 collects concluding remarks and points out some possible research lines.

Notation. We denote the set of natural numbers by $\mathbb{N}$, the vector space of n_x-by-n_y real matrices by $\mathbb{R}^{n_x\times n_y}$ and the subspace of symmetric matrices by $\mathbb{S}^{n_x}\in\mathbb{R}^{n_x\times n_x}$ where the multiplicative and additive identities are denoted by $I_{n_x}\in\mathbb{S}^{n_x}$ and $0_{n_x,n_y}\in\mathbb{R}^{n_x\times n_y}$, respectively. The superscript "T" denotes matrix transposition, "$\otimes$" the Kronecker product, diag (...) a block-diagonal matrix, $\mathrm{H_e}\{P\}=P+P^T$ the Hermitian operator applied to matrix P, $\partial_t x(z,t)$, $\partial_z x(z,t)$ and $\partial_z^2 x(z,t)$ the time, first and second order spatial derivatives of the function $x(z,t)$, with respect to z, respectively. $\mathbf{L}_2^{n_x}(0,1)$ denotes the space of square Lebesgue integrable n_x-dimensional vector valued functions, that is, functions with finite norm

$$\|x(\cdot,t)\|_2=\langle x(\cdot,t),x(\cdot,t)\rangle^{\frac{1}{2}}=\left(\int_0^1 x^T(z,t)x(z,t)dz\right)^{\frac{1}{2}}.$$

$Z_m(z)$ denotes the vector of monomial bases of degree m or less, i.e.,

$$Z_m(z)=\begin{bmatrix}1 & z & \cdots & z^{m-1} & z^m\end{bmatrix}^T, \tag{1}$$

the sets $\{1,\dots,n_x\}$ and $\{1,\dots,n_y\}$ are denoted by $\mathbb{N}_{n_x}$ and $\mathbb{N}_{n_y}$ respectively and $1_{[a,b]}(z)$ is the characteristic function of the interval $[a,b]$, that is,

$$1_{[a,b]}(z)=\begin{cases}1, & a\le z\le b,\\ 0, & \text{elsewhere}.\end{cases} \tag{2}$$

Instrumental Tools and Definitions. The following definition and useful results will be instrumental to derive the main results of this paper.

Definition 1. Let $x,\ \hat{x}\in\mathbb{R}^{n_x}$. We define by $Co(x,\hat{x})$ the convex hull of the set $\{x,\ \hat{x}\}$, i.e.

$$Co(x,\hat{x})=\{\theta x+(1-\theta)\hat{x}:\ \theta\in[0,1]\}. \tag{3}$$

Lemma 1 (*Differential Mean Value Theorem [24]*)**.** *Let the function $r(x):\mathbb{R}^{n_x}\to\mathbb{R}^{n_r}$ differentiable with respect to x and let $x,\ \hat{x}$ be two elements in $\mathbb{R}^n$. Then, there is an element $\breve{x}\in Co(x,\hat{x})$, such that:*

$$r(x)-r(\hat{x})=\nabla r(\breve{x})(x-\hat{x}) \tag{4}$$

where $\nabla r=\begin{bmatrix}\partial_{x_1}r & \cdots & \partial_{x_n}r\end{bmatrix}$.

Lemma 2 (*Wirtinger's Inequality [25]*)**.** *For the vector function $x(z,t)$ whose elements are absolutely continuous scalar functions with respect to z such that $\partial_z x(z,t)\in\mathbf{L}_2^{n_x}(0,1)$ with $x(a,t)=0$ or $x(b,t)=0$, the following inequality holds*

$$\int_a^b x^T(z,t)x(z,t)dz\le \frac{4(b-a)^2}{\pi^2}\int_a^b \partial_z x^T(z,t)\partial_z x(z,t)dz. \tag{5}$$

2. System description

Consider a transport-reaction system described by the following semilinear parabolic PDE:

$$\partial_t x(z,t)=D\partial_z^2 x(z,t)-\mathcal{V}\partial_z x(z,t)-Kx(z,t)+B\,u_d(t)+G\,r\,(x(z,t)) \tag{6}$$

for $(z,t)\in(0,1)\times(0,\infty)$, subject to Robin boundary conditions

$$\begin{aligned}M_{\alpha_0}\partial_z x(0,t)+M_{\beta_0}x(0,t)&=u_0(t)\\ M_{\alpha_1}\partial_z x(1,t)+M_{\beta_1}x(1,t)&=u_1(t)\end{aligned} \tag{7}$$

for $t\in[0,\infty)$, where

$$x(\cdot,t)=\begin{bmatrix}x_1(\cdot,t) & \cdots & x_{n_x}(\cdot,t)\end{bmatrix}^T\in\mathbf{L}_2^{n_x}(0,1)$$

denotes the state variable,

$$u_d(t)=\begin{bmatrix}u_{d,1}(t) & \cdots & u_{d,n_x}(t)\end{bmatrix}^T\in\mathbb{R}^{n_d}$$

is a known distributed exogenous input and

$$u_0(t)=\begin{bmatrix}u_{0,1}(t), & \cdots & u_{0,n_x}(t)\end{bmatrix}^T\in\mathbb{R}^{n_x}$$
$$u_1(t)=\begin{bmatrix}u_{1,1}(t) & \cdots & u_{1,n_x}(t)\end{bmatrix}^T\in\mathbb{R}^{n_x}$$

are the known boundary exogenous inputs at $z=0$ and $z=1$, respectively. The matrices $D=\mathrm{diag}(d_i)$, $\mathcal{V}=\mathrm{diag}(\upsilon_i)$, $i=1,\dots,n_x$, have constant entries denoting the diffusion coefficients and superficial velocities, respectively, $K\in\mathbb{R}^{n_x\times n_x}$ is the linear source matrix, $B\in\mathbb{R}^{n_x\times n_d}$ is the shaping distributed input matrix, $G\in\mathbb{R}^{n_x\times n_r}$ is the kinetic gain matrix and $r(\cdot):\mathbf{L}_2^{n_x}(0,1)\to\mathbf{L}_2^{n_r}(0,1)$ is the vector of reaction rates. The matrices $M_{\alpha_0}=\mathrm{diag}(\alpha_{0,i})$, $M_{\beta_0}=\mathrm{diag}(\beta_{0,i})$, $M_{\alpha_1}=\mathrm{diag}(\alpha_{1,i})$ and $M_{\beta_1}=\mathrm{diag}(\beta_{1,i})$, $i=1,\dots,n_x$, have constant entries denoting the coefficients related to Robin boundary conditions.

In this work, we are concerned in designing a state observer for the transport-reaction system described by (6) from a finite number of spatially distributed measurements. The following will be assumed to ensure the well-posedness of the governing equations and the observer design problem.

- $d_i\ge D_{\min}>0$, for $i=1,\dots,n_x$.
- $r(\cdot):\mathbf{L}_2^{n_x}(0,1)\to\mathbf{L}_2^{n_r}(0,1)$ is locally Lipschitz continuous in x, i.e., there exists a positive constant $l^r=l^r(\rho)$ such that

$$\|r(x)-r(\hat{x})\|\le l^r\|x-\hat{x}\| \tag{8}$$

holds for all $x,\hat{x}\in\mathbf{L}_2^{n_x}(0,1)$ with ρ being a positive scalar such that $\|x\|<\rho$ and $\|\hat{x}\|\le\rho$ hold.

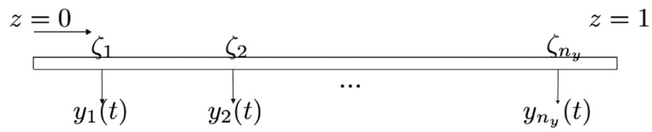

Fig. 1. Distributed pointwise measurements.

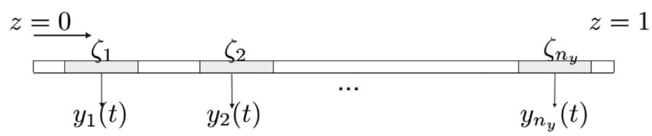

Fig. 2. Distributed piecewise measurements.

- $\alpha_{0,i}$, $\alpha_{1,i}$ are not all zero in such a way that mixed Dirichlet and Neumann boundary conditions may coexist.

2.1. Output measurement

In this work, the measurement vector of the system described in (6)–(7) is assumed to be defined as follows

$$y(t)=\begin{bmatrix}\int_0^1 c_1(z)\mathbf{c}_1^T x(z,t)dz\\ \vdots \\ \int_0^1 c_{n_y}(z)\mathbf{c}_{n_y}^T x(z,t)dz\end{bmatrix}\in\mathbb{R}^{n_y} \tag{9}$$

where $c_j(z)\in\mathbb{R}$, $j\in\mathbb{N}_{n_y}$, describes the distribution of the measurement at the jth position over the spatial domain $[0,1]$ and $\mathbf{c}_j\in\mathbb{R}^{n_x}$, $j\in\mathbb{N}_{n_y}$, is a vector defining the measured variable around that position.

Measurement sensors in a number of practical problems are only placed at a finite number of discrete points or partial areas of the spatial domain. Different shape functions $c_j(z)$ will lead to different forms of local measurement. For instance, the following definition

$$c_j(z)=\delta(z-\zeta_j),\quad j\in\mathbb{N}_{n_y}, \tag{10}$$

corresponds to pointwise measurement at position ζ_j, $j\in\mathbb{N}_{n_y}$, while the functional form

$$c_j(z)=\frac{1}{2\varepsilon_j}1_{[\zeta_j-\varepsilon_j,\zeta_j+\varepsilon_j]} \tag{11}$$

with

$$1_{[\zeta_j-\varepsilon_j,\zeta_j+\varepsilon_j]}=\begin{cases}1, & \text{if } z\in[\zeta_j-\varepsilon_j,\zeta_j+\varepsilon_j],\\ 0, & \text{elsewhere}\end{cases} \tag{12}$$

produces n_y zones of piecewise uniform sensing in the interval $[\zeta_j-\varepsilon_j,\zeta_j+\varepsilon_j]$, for all $j\in\mathbb{N}_{n_y}$. These cases are illustrated in Figs. 1 and 2, respectively.

3. Observer design — Instrumental tools

Consider the following Luenberger-like state observer for (6)–(7):

$$\begin{aligned}\partial_t\hat{x}(z,t)&=D\partial_z^2\hat{x}(z,t)-\mathcal{V}\partial_z\hat{x}(z,t)\\ &\quad-K\hat{x}(z,t)+B\,u_d(t)+G\,r(\hat{x}(z,t))\\ &\quad+L_D(z)\left(y(t)-\hat{y}(t)\right)\end{aligned} \tag{13}$$

for $(z,t)\in(0,1)\times(0,\infty)$, subject to

$$M_{\alpha_0}\partial_z\hat{x}(0,t)+M_{\beta_0}\hat{x}(0,t)=u_0(t) \tag{14}$$

$$M_{\alpha_1}\partial_z\hat{x}(1,t)+M_{\beta_1}\hat{x}(1,t)=u_1(t) \tag{15}$$

and the initial condition

$$\hat{x}_0(z)=\hat{x}(z,0) \tag{16}$$

for $z\in[0,1]$. Here $L_D:[0,1]\to\mathbb{R}^{n_x\times n_y}$ is the output injection gain to be designed.

Let

$$e(z,t)=x(z,t)-\hat{x}(z,t) \tag{17}$$

be the estimation error vector. Then, the estimation error dynamics is given by

$$\begin{aligned}\partial_t e(z,t)&=D\partial_z^2 e(z,t)-\mathcal{V}\partial_z e(z,t)\\ &\quad-Ke(z,t)+G\left[r\left(x(z,t)\right)-r\left(\hat{x}(z,t)\right)\right]\\ &\quad-L_D(z)\left(y(t)-\hat{y}(t)\right)\end{aligned} \tag{18}$$

subject to

$$M_{\alpha_0}\partial_z e(0,t)+M_{\beta_0}e(0,t)=0 \tag{19}$$

$$M_{\alpha_1}\partial_z e(1,t)+M_{\beta_1}e(1,t)=0 \tag{20}$$

and the initial condition

$$e_0(z)=e(z,0). \tag{21}$$

In the sequel, the output injection gain is designed using a Lyapunov-based technique in order to obtain sufficient conditions guaranteeing the stability of the estimation error dynamics described by (18)–(21). To this end, based on the assumption that $r(\cdot)$ is locally Lipschitz, notice that the function denoted as

$$\nu(z,t)=r(x(z,t))-r(\hat{x}(z,t)) \tag{22}$$

and the estimation error $e(z,t)$ satisfy different algebraic conditions [26]. Hence, to deal with the term $\nu(z,t)$, a sector condition based on the boundedness of the Jacobian matrix of the nonlinear function $r(\cdot)$ will be considered.

3.1. Sector condition

Let $\Gamma_1,\ \Gamma_2\in\mathbb{R}^{n_r\times n_x}$ be two constant matrices whose entries are the local lower and upper bounds, respectively, of the Jacobian matrix entries of $r(\cdot)$, which is defined as

$$\Gamma(x(z,t))=\nabla r(x(z,t)). \tag{23}$$

By the virtue of Lemma 1, we obtain

$$\nu(z,t)=\nabla r\left(\check{x}(z,t)\right)e(z,t) \tag{24}$$

where $\check{x}(z,t)\in Co(x(z,t),\hat{x}(z,t))$. Thus, the following inequality holds

$$\Gamma_1\,e(z,t)\le\nu(z,t)\le\Gamma_2\,e(z,t) \tag{25}$$

and the following sector condition can be straightforwardly obtained

$$\left(\nu(z,t)-\Gamma_1 e(z,t)\right)^T\left(\Gamma_2 e(z,t)-\nu(z,t)\right)\ge 0 \tag{26}$$

leading to

$$\left\langle\begin{bmatrix}e(z,t)\\ \nu(z,t)\end{bmatrix},\underbrace{\begin{bmatrix}\frac{\Gamma_1^T\Gamma_2+\Gamma_2^T\Gamma_1}{2} & -\frac{\Gamma_1^T+\Gamma_2^T}{2}\\ -\frac{\Gamma_1+\Gamma_2}{2} & I_{n_r}\end{bmatrix}}_{M}\begin{bmatrix}e(z,t)\\ \nu(z,t)\end{bmatrix}\right\rangle\le 0 \tag{27}$$

3.2. Abstract formulation

The error dynamics described by (18)–(21) can be rewritten as an abstract first order ordinary differential equation in the Hilbert space $\mathcal{H}=\mathbf{L}_2^{n_x}(0,1)$ according to

$$\begin{aligned}\partial_t e(z,t)&=(\mathcal{A}-L_D(z)\mathcal{C})e(z,t)+G\nu(z,t),\\ e(z,0)&=e_0(z)\in\mathcal{H}\end{aligned} \tag{28}$$

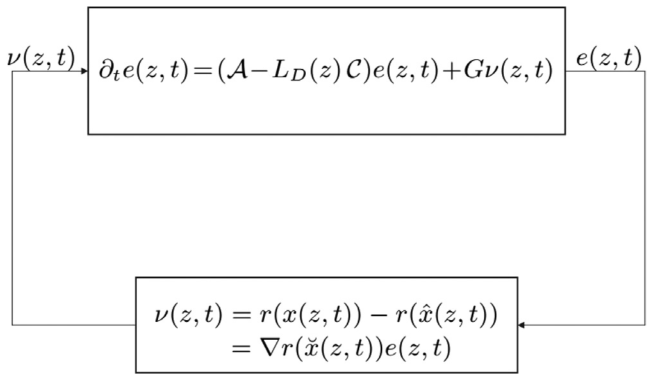

Fig. 3. Lure-System representation of the error dynamics.

where the operators $\mathcal{A} : D(\mathcal{A}) \to \mathcal{H}$, $\mathcal{C} : D(\mathcal{C}) \to \mathbb{R}^{n_y}$ are defined as

$$\mathcal{A}e(z,t) = D\partial_z^2 e(z,t) - \mathcal{V}\partial_z e(z,t) - Ke(z,t)$$
$$D(\mathcal{A}) = \{e(z,t) \in \mathcal{H} : e(z,t),\ \partial_z e(z,t) \text{ are absolutely continuous, } \partial_z^2 e(z,t) \in \mathcal{H} \text{ and } M_{\alpha_0}\partial_z e(0,t) + M_{\beta_0} e(0,t) = 0,\ M_{\alpha_1}\partial_z e(1,t) + M_{\beta_1} e(1,t) = 0\}.$$
$$\mathcal{C}e(z,t) = \begin{bmatrix} \langle c_1(\cdot), \mathbf{c}_1^T e(\cdot,t)\rangle \\ \vdots \\ \langle c_{n_y}(\cdot), \mathbf{c}_{n_y}^T e(\cdot,t)\rangle \end{bmatrix}.$$

The error dynamics in (28) can be represented as a Lure system, depicted in Fig. 3, where the sector condition for the estimation error $e(t)$ and the deviation function $\nu(t)$ are expressed through the scalar constraint (27) that can be embedded into the stability analysis by applying the S-Procedure [27].

3.3. Lyapunov convergence analysis

The state estimation convergence is evaluated within a weighted Lyapunov framework, with the weight function as a degree of freedom [15]. The analysis of the corresponding dissipation mechanism leads to an LMI condition, which depends on the spatial coordinate, the observer gain, and the Lyapunov weight functional.

To this end, let $V : \mathbf{L}_2^{n_x}(0,1) \to \mathbb{R}$ be the (positive definite) weight functional candidate as defined below:

$$V(t) = \langle e(\cdot,t), \mathcal{P}e(\cdot,t)\rangle \tag{29}$$

where $\mathcal{P} : \mathbf{L}_2^{n_x}(0,1) \to \mathbf{L}_2^{n_x}(0,1)$ is a strictly positive operator defined by a polynomial matrix $W(z)$ (to be defined later in this section) as follows:

$$(\mathcal{P}e)(z) = W(z)e(z). \tag{30}$$

for all $z \in (0,1)$.

The following Lemma shows how two positive semi-definite matrices Q and R, and a positive scalar ϵ can be used to define the polynomial matrix $W(z)$ such that the operator $\mathcal{P}$ is positive and therefore the functional $V(t)$ is a Lyapunov candidate for the estimation error dynamics (18)–(21).

Lemma 3 (*[18,23]*)**.** *Let $Q,\ R \in \mathbb{S}^{n_x(m+1)}$ be positive semi-definite matrices, and define*

$$Z(z) = Z_m(z) \otimes I_{n_x}, \tag{31}$$

$$g(z) = z(1-z), \tag{32}$$

and

$$W(z) = Z(z)^T(Q + g(z)R)Z(z) + \epsilon I_{n_x}, \tag{33}$$

for some $\epsilon > 0$, where $z \in [0,1]$, Z_m is a vector of monomials with a degree equal to or smaller than m and $\otimes$ stands for the Kronecker product.

Then, the functional $V : \mathbf{L}_2^{n_x}(0,1) \to \mathbb{R}$, defined as

$$V(e(\cdot,t)) = \langle e(\cdot,t), \mathcal{P}e(\cdot,t)\rangle = \int_0^1 e(z,t)^T W(z) e(z,t)dz, \tag{34}$$

is strictly positive over $\mathbf{L}_2^{n_x}(0,1)$, for $e(\cdot,t) \neq 0$, and satisfies

$$V(e(\cdot,t)) = \langle e(\cdot,t), \mathcal{P}e(\cdot,t)\rangle \geq \epsilon\|e(\cdot,t)\|^2,\quad \forall\ e(\cdot,t) \in \mathbf{L}_2^{n_x}(0,1). \tag{35}$$

In order to design the observer gain $L_D(z)$, consider the following dissipation inequality:

$$\dot{V}(t) + 2\gamma V(t) \leq 0, \tag{36}$$

where γ is a positive scalar. If (36) is satisfied along the trajectories of the estimation error dynamics (28), the estimation error dynamics is exponentially stable with a guaranteed decay rate γ, since it can be readily shown that the following holds

$$\|e(\cdot,t)\| \leq M_e(e_0)\mathrm{e}^{-\gamma t}, \tag{37}$$

where

$$M_e(e_0) = \sqrt{\frac{V\ (e_0(z))}{\epsilon}}. \tag{38}$$

Next, substituting (29) and (30) into (36), it follows that

$$\dot{V}(t) + 2\gamma V(t) = \langle \partial_t e(\cdot,t), \mathcal{P}e(\cdot,t)\rangle + \langle e(\cdot,t), \mathcal{P}\partial_t e(\cdot,t)\rangle + 2\gamma\langle e(\cdot,t), \mathcal{P}e(\cdot,t)\rangle. \tag{39}$$

Using the self-adjointness of $\mathcal{P}$, (39) can be cast as follows

$$\dot{V}(t) + 2\gamma V(t) = 2\langle e(\cdot,t), P\partial_t e(\cdot,t)\rangle + 2\gamma\langle e(\cdot,t), \mathcal{P}e(\cdot,t)\rangle, \tag{40}$$

which along the trajectories of the error dynamics (28) leads to

$$\dot{V}(t) + 2\gamma V(t) = 2\langle e(\cdot,t), \mathcal{P}\mathcal{A}e(\cdot,t)\rangle + 2\langle e(\cdot,t), \mathcal{P}G\nu(z,t)\rangle - 2\langle e(\cdot,t), \mathcal{P}L_D(z)\mathcal{C}e(\cdot,t)\rangle + 2\gamma\langle e(\cdot,t), \mathcal{P}e(\cdot,t)\rangle. \tag{41}$$

In the following section, the dissipation inequality in (36) considering (41) is recast in terms of parameterized LMI constraints which can be solved using standard sum of squares (SOS) tools [20].

4. Observer design — Main result

In this section, an LMI formulation of the distributed observation problems is developed. The local exponential stability of the estimation error system (18)–(21) is ensured for two cases of in domain distributed measurement: pointwise measurement and piecewise measurement.

4.1. Pointwise measurements at $\zeta_j,\ \forall j \in \mathbb{N}_{n_y}$

In this case, as shown in Fig. 4, we divide the spatial domain $[0,1]$ into n_y subintervals $[\tilde{z}_j, \tilde{z}_{j+1}]$, $j \in \mathbb{N}_{n_y}$ according to the

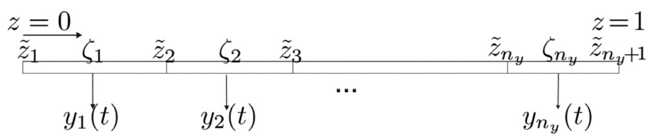

Fig. 4. Distributed pointwise measurements.

position of the measurement sensors. From Fig. 4, we get that $0 = \tilde{z}_1 < \cdots < \tilde{z}_{n_y+1} = 1$ and

$$\zeta_j \in [\tilde{z}_j, \tilde{z}_{j+1}], \quad \forall j \in \mathbb{N}_{n_y}. \tag{42}$$

Remark 1. For a given set of pointwise measurements at $\{\zeta_j : j \in \mathbb{N}_{n_y}\}$, the selection of the auxiliary set $\{\tilde{z}_j : j = 2, \ldots, n_y\}$ is a degree of freedom for the solution of the observer design problem, i.e., different configurations according to Fig. 4 may lead to different feasible solutions and observer performance.

Theorem 1. *The error dynamics in (18)–(21), with $c_j(z)$, $j \in \mathbb{N}_{n_y}$, given by (10), is exponentially stable with a guaranteed decay rate γ, if there exist*

- *m, $q \in \mathbb{N}$, and real positive scalars ϵ, τ;*
- *either positive semidefinite matrices Q, $R \in \mathbb{S}^{n_x(m+1)}$ (for the equi-diffusivity and equi-advectivity case, i.e., $D = dI_{n_x}$ and $\mathcal{V} = \upsilon I_{n_x}$) or diagonal matrices Q, $R \in \mathbb{S}^{n_x(m+1)}$ such that the polynomial matrix $W : [0, 1] \to \mathbb{R}^{n_x \times n_x}$ satisfies (33); and*
- *qth degree polynomials $l_j : [0, 1] \to \mathbb{R}^{n_x}$, $\forall j \in \mathbb{N}_{n_y}$ defining the observer gain*

$$L_D(z) = \left[1_{[\tilde{z}_1, \tilde{z}_2]} l_1(z) \;\; \cdots \;\; 1_{[\tilde{z}_{n_y}, \tilde{z}_{n_y+1}]} l_{n_y}(z) \right], \tag{43}$$

such that the following matrix inequalities hold:

$$\begin{aligned} &2\tilde{D}(1)M_{\alpha_1}^{-1}M_{\beta_1} + \partial_z\tilde{D}(1) + \tilde{\mathcal{V}}(1) \geq 0 \\ &2\tilde{D}(0)M_{\alpha_0}^{-1}M_{\beta_0} + \partial_z\tilde{D}(0) + \tilde{\mathcal{V}}(0) \leq 0 \end{aligned} \tag{44}$$

$$P_j(z) - \tau \begin{bmatrix} M & 0_{(n_x+n_r),n_x} \\ * & 0_{n_x} \end{bmatrix} \leq 0 \tag{45}$$

$\forall j \in \mathbb{N}_{n_y}$ and $z \in [0, 1]$, where

$$P_j(z) = \begin{bmatrix} \Pi_j(z) & \tilde{G}(z) & \frac{\pi^2\epsilon}{2p_j^2} I_{n_x} - \tilde{l}_j(z)\mathbf{c}_j^T \\ * & 0_{n_r} & 0_{n_r,n_x} \\ * & * & -\frac{\pi^2\epsilon D_{min}}{2p_j^2} I_{n_x} \end{bmatrix} \tag{46}$$

with

$$\begin{aligned} \Pi_j(z) = {} & \partial_z^2\tilde{D}(z) + \partial_z\tilde{\mathcal{V}}(z) - \tilde{K}(z) \\ & - \frac{\pi^2\epsilon D_{min}}{2p_j^2} I_{n_x} + 4\gamma W(z) \end{aligned} \tag{47}$$

$$\begin{aligned} &\tilde{D}(z) = W(z)D, && \tilde{\mathcal{V}}(z) = W(z)\mathcal{V}, \\ &\tilde{K}(z) = \mathrm{H_e}\{W(z)K\}, && \tilde{G}(z) = W(z)G, \\ &\tilde{l}_j(z) = W(z)l_j(z), && D_{\min} = \min_{\forall i \in \mathbb{N}_{n_x}} d_i, \\ &p_j^2 = \max\{(\zeta_j - \tilde{z}_j)^2, (\tilde{z}_{j+1} - \zeta_j)^2\}, \;\; \forall j \in \mathbb{N}_{n_y}. \end{aligned}$$

Proof. Consider the linear dissipation expression of the Lyapunov function given in (41) with $L_D(z)$ as defined in (43). Then, substituting (18) into (41) yields

$$\begin{aligned} \dot{V}(t) + 2\gamma V(t) = {} & 2\int_0^1 \left\{ e^T(z,t)W(z) \left\{ D\partial_z^2 e(z,t) \right.\right. \\ & \left.\left. - \mathcal{V}\partial_z e(z,t) - (K - \gamma I_{n_x})e(z,t) \right\} dz \right\} \\ & + 2\int_0^1 e^T(z,t)W(z)G\nu(z,t)dz \\ & -2\sum_{j=1}^{n_y} \int_{\tilde{z}_j}^{\tilde{z}_{j+1}} e^T(z,t)W(z)l_j(z)\mathbf{c}_j^T e(\zeta_j,t)dz. \end{aligned} \tag{48}$$

Regarding the definitions of $\tilde{D}(z)$, $\tilde{\mathcal{V}}(z)$, $\tilde{K}(z)$, $\tilde{G}(z)$ and $\tilde{l}_j(z)$ in (47), we must recall the constraints on the definitions of $Q, R, \tilde{D}(z)$, and $\tilde{\mathcal{V}} : [0, 1] \to \mathbb{S}^{n_x}$. Hence, in order to apply the integration by parts in (48), we take (74) and (77) into account as presented in Appendix. Thus, (48) becomes

$$\begin{aligned} \dot{V}(t) + 2\gamma V(t) = {} & -e^T(1,t) \left\{ 2\tilde{D}(1)M_{\alpha_1}^{-1}M_{\beta_1} \right. \\ & \left. + \partial_z\tilde{D}(1) + \tilde{\mathcal{V}}(1) \right\} e(1,t) \\ & + e^T(0,t)\left[2\tilde{D}(0)M_{\alpha_0}^{-1}M_{\beta_0} + \partial_z\tilde{D}(0) + \tilde{\mathcal{V}}(0) \right] e(0,t) \\ & - 2\int_0^1 \partial_z e^T(z,t)\tilde{D}(z)\partial_z e(z,t)dz \\ & + 2\int_0^1 e^T(z,t)\tilde{G}(z)\nu(z,t)dz \\ & + \int_0^1 \left\{ e^T(z,t) \left\{ \partial_z^2\tilde{D}(z) + \partial_z\tilde{\mathcal{V}}(z) - \tilde{K}(z) \right.\right. \\ & \left.\left. + 2\gamma W(z) \right\} e(z,t)dz \right\} \\ & - 2\sum_{j=1}^{n_y} \int_{\tilde{z}_j}^{\tilde{z}_{j+1}} e^T(z,t)\tilde{l}_j(z)\mathbf{c}_j^T e(\zeta_j,t)dz. \end{aligned} \tag{49}$$

Notice by the virtue of Wirtinger's inequality that the following hold

$$\begin{aligned} & -\int_{\tilde{z}_j}^{\zeta_j} \partial_z e^T(z,t)\tilde{D}(z)\partial_z e(z,t)dz \leq \\ & \frac{-\pi^2\epsilon D_{min}}{4(\zeta_j - \tilde{z}_j)^2} \int_{\tilde{z}_j}^{\zeta_j} e^{(j)}(z,t)^T e^{(j)}(z,t)dz \end{aligned} \tag{50}$$

$$\begin{aligned} & -\int_{\zeta_j}^{\tilde{z}_{j+1}} \partial_z e^T(z,t)\tilde{D}(z)\partial_z e(z,t)dz \leq \\ & \frac{-\pi^2\epsilon D_{min}}{4(\tilde{z}_{j+1} - \zeta_j)^2} \int_{\zeta_j}^{\tilde{z}_{j+1}} e^{(j)}(z,t)^T e^{(j)}(z,t)dz. \end{aligned} \tag{51}$$

where

$$e^{(j)}(z,t) = e(z,t) - e(\zeta_j,t).$$

Next, summing up (50) and (51) leads to

$$\begin{aligned} & -\int_{\tilde{z}_j}^{\tilde{z}_{j+1}} \partial_z e^T(z,t)\tilde{D}(z)\partial_z e(z,t)dz \leq \\ & - \frac{\pi^2\epsilon D_{min}}{4p_j^2} \int_{\tilde{z}_j}^{\tilde{z}_{j+1}} e^T(z,t)e(z,t)dz \\ & + \frac{\pi^2\epsilon D_{min}}{2p_j^2} \int_{\tilde{z}_j}^{\tilde{z}_{j+1}} e^T(z,t)e(\zeta_j,t)dz \\ & - \frac{\pi^2\epsilon D_{min}}{4p_j^2} \int_{\tilde{z}_j}^{\tilde{z}_{j+1}} e^T(\zeta_j,t)e(\zeta_j,t)dz \end{aligned} \tag{52}$$

Hence, substituting (52) into (49) yields

$$\begin{aligned} & \dot{V}(t) + 2\gamma V(t) \leq \\ & - e^T(1,t)\left[2\tilde{D}(1)M_{\alpha_1}^{-1}M_{\beta_1} + \partial_z\tilde{D}(1) + \tilde{\mathcal{V}}(1) \right] e(1,t) \\ & + e^T(0,t)\left[2\tilde{D}(0)M_{\alpha_0}^{-1}M_{\beta_0} + \partial_z\tilde{D}(0) + \tilde{\mathcal{V}}(0) \right] e(0,t) \end{aligned}$$

$$+\sum_{j=1}^{n_y}\left[\int_{\tilde z_j}^{\tilde z_{j+1}}\left[e^T(z,t)\left[\partial_z^2\tilde D(z)+\partial_z\tilde{\mathcal V}(z)-\tilde K(z)\right.\right.\right.$$
$$\left.\left.\left.-\frac{\pi^2\epsilon D_{min}}{2p_j^2}I_{n_x}+2\gamma W(z)\right]e(z,t)dz\right]\right]$$
$$+2\sum_{j=1}^{n_y}\int_{\tilde z_j}^{\tilde z_{j+1}}e^T(z,t)\tilde G(z)\nu(z,t)dz$$
$$-\sum_{j=1}^{n_y}\frac{\pi^2\epsilon D_{min}}{2p_j^2}\int_{\tilde z_j}^{\tilde z_{j+1}}e^T(\zeta_j,t)e(\zeta_j,t)dz$$
$$+\sum_{j=1}^{n_y}\frac{\pi^2\epsilon D_{min}}{p_j^2}\int_{\tilde z_j}^{\tilde z_{j+1}}e^T(z,t)e(\zeta_j,t)dz$$
$$-2\sum_{j=1}^{n_y}\int_{\tilde z_j}^{\tilde z_{j+1}}e^T(z,t)\tilde l_j(z)\mathbf{c}_j^Te(\zeta_j,t)dz, \tag{53}$$

which can be cast as follows

$$\dot V(t)+2\gamma V(t)\le$$
$$-\ e^T(1,t)\left[2\tilde D(1)M_{\alpha_1}^{-1}M_{\beta_1}+\partial_z\tilde D(1)+\tilde{\mathcal V}(1)\right]e(1,t)$$
$$+\ e^T(0,t)\left[2\tilde D(0)M_{\alpha_0}^{-1}M_{\beta_0}+\partial_z\tilde D(0)+\tilde{\mathcal V}(0)\right]e(0,t)$$
$$+\sum_{j=1}^{n_y}\int_{\tilde z_j}^{\tilde z_{j+1}}\mathbf{e}^T(z,t)P_j(z)\mathbf{e}(z,t)dz \tag{54}$$

where $\mathbf{e}_j(z,t)=[e(z,t)\ \ \nu(z,t)\ \ e(\zeta_j,t)]^T$.

Therefore, in order to ensure the negativity of the right-hand side of (54), it suffices that

$$\begin{aligned}&2\tilde D(1)M_{\alpha_1}^{-1}M_{\beta_1}+\partial_z\tilde D(1)+\tilde{\mathcal V}(1)\ge 0\\&2\tilde D(0)M_{\alpha_0}^{-1}M_{\beta_0}+\partial_z\tilde D(0)+\tilde{\mathcal V}(0)\le 0\end{aligned} \tag{55}$$

and

$$P_j(z)\le 0,\ \ \forall j\in\mathbb N_{n_y}. \tag{56}$$

Applying the S-procedure to (56) and (27), we obtain

$$P_j(z)-\tau\begin{bmatrix}M & 0_{(n_x+n_r),n_x}\\ * & 0_{n_x}\end{bmatrix}\le 0,\ \ \forall j\in\mathbb N_{n_y}. \tag{57}$$

Then, (55) and (57) imply that $V(t)\le e^{-2\gamma t}V(0)$ and (37) taking Section 3.3 into account, which completes the proof. □

4.2. Piecewise measurements

In this case, as shown in Fig. 5, the spatial domain [0, 1] is divided into n_y subintervals $[\tilde z_j,\tilde z_{j+1}]$, $j\in\mathbb N_{n_y}$, according to the position of the measurement sensors. Also, from Fig. 5, notice that $0=\tilde z_1<\cdots<\tilde z_{n_y+1}=1$ and

$$[\zeta_j-\varepsilon_j,\zeta_j+\varepsilon_j]\subset[z_j,z_{j+1}],\quad\forall\, j\in\mathbb N_{n_y}, \tag{58}$$

with the scalars $\varepsilon_1,\ldots,\varepsilon_{n_y}$ being such that

$$\zeta_j-\varepsilon_j<\tilde z_j\ \text{ and }\ \zeta_j+\varepsilon_j<\tilde z_{j+1},\ j\in\mathbb N_{n_y},$$

to avoid overlapping among the measurement intervals.

Theorem 2. *The error dynamics in (18)–(21), with $c_j(z)$, $j\in\mathbb N_{n_y}$, given by (11), is exponentially stable with a guaranteed decay rate γ, if the conditions in Theorem 1 are satisfied with p_j, $j\in\mathbb N_{n_y}$, in (47) being redefined as follows:*

$$p_j^2=\max\{(\zeta_j+\varepsilon_j-\tilde z_j)^2,(\tilde z_{j+1}-\zeta_j+\varepsilon_j)^2\},\quad\forall\, j\in\mathbb N_{n_y}. \tag{59}$$

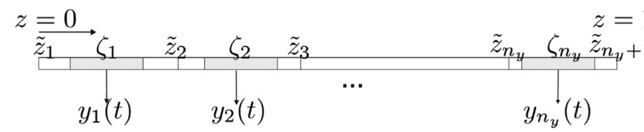

Fig. 5. Distributed piecewise measurements.

Proof. This proof follows similar steps to the proof of Theorem 1. Thus, the linear dissipation expression of the Lyapunov function given in (41) along (18) can be expressed as follows:

$$\dot V(t)+2\gamma V(t)=2\int_0^1\left[e^T(z,t)W(z)\left[D\partial_z^2e(z,t)\right.\right.$$
$$\left.\left.-\mathcal V\partial_ze(z,t)-(K-\gamma I_{n_x})e(z,t)\right]dz\right]$$
$$+2\int_0^1e^T(z,t)W(z)G\nu(z,t)dz$$
$$-2\sum_{j=1}^{n_y}\int_{\tilde z_j}^{\tilde z_{j+1}}e^T(z,t)W(z)l_j(z)\mathbf{c}_j^Te(\bar\zeta_j^t,t)dz \tag{60}$$

where $e(\bar\zeta_j^t,t)$ corresponds to the application of the first mean value theorem for integration, since for each $j\in\mathbb N_{n_y}$ and any $t\ge 0$, there exists a scalar $\bar\zeta_j^t\in[\zeta_j-\epsilon_j,\zeta_j+\epsilon_j]$ such that

$$\frac{1}{2\epsilon_j}\int_{\zeta_j-\varepsilon_j}^{\zeta_j+\varepsilon_j}e(z,t)dz=e(\bar\zeta_j^t,t) \tag{61}$$

holds.

Regarding the definitions of $\tilde D(z)$, $\tilde{\mathcal V}(z)$, $\tilde K(z)$, $\tilde G(z)$ and $\tilde l_j(z)$ in (47) and applying the integration by parts into (60), we obtain (49) where $e(\zeta_j,t)$ is now substituted by $e(\tilde\zeta_j^t,t)$. Hence, by applying the Wirtinger's lemma, it follows that:

$$\begin{aligned}&-\int_{\tilde z_j}^{\tilde\zeta_j^t}\partial_ze^T(z,t)\tilde D(z)\partial_ze(z,t)dz\le\\&\frac{-\pi^2\epsilon D_{min}}{4(\tilde\zeta_j^t-\tilde z_j)^2}\int_{\tilde z_j}^{\tilde\zeta_j^t}e^j(z,t)^Te^{(j)}(z,t)dz\end{aligned} \tag{62}$$

$$\begin{aligned}&-\int_{\tilde\zeta_j^t}^{\tilde z_{j+1}}\partial_ze^T(z,t)\tilde D(z)\partial_ze(z,t)dz\le\\&\frac{-\pi^2\epsilon D_{min}}{4(\tilde z_{j+1}-\tilde\zeta_j^t)^2}\int_{\tilde\zeta_j^t}^{\tilde z_{j+1}}e^j(z,t)^Te^j(z,t)dz.\end{aligned} \tag{63}$$

where

$$D_{\min}=\min_{\forall\ i\in\mathbb N_{n_x}}d_i\ \text{ and }\ e^{(j)}(z,t)=e(z,t)-e(\tilde\zeta_j^t,t).$$

Since $\tilde\zeta_j^t\in[\zeta_j-\varepsilon_j,\zeta_j+\varepsilon_j]\subset[z_j,z_{j+1}]$, $\forall\, j\in\mathbb N_{n_y}$ and $t\ge 0$, we obtain

$$\tilde\zeta_j^t-\tilde z_j\le\zeta_j+\varepsilon_j-\tilde z_j,\quad\tilde z_{j+1}-\tilde\zeta_j^t\le\tilde z_{j+1}-\zeta_j+\varepsilon_j \tag{64}$$

Next, summing up (62) and (63) yields

$$-\int_{\tilde z_j}^{\tilde z_{j+1}}\partial_ze^T(z,t)\tilde D(z)\partial_ze(z,t)dz\le$$
$$-\frac{\pi^2\epsilon D_{min}}{4p_j^2}\int_{\tilde z_j}^{\tilde z_{j+1}}e^T(z,t)e(z,t)dz$$
$$+\frac{\pi^2\epsilon D_{min}}{2p_j^2}\int_{\tilde z_j}^{\tilde z_{j+1}}e^T(z,t)e(\tilde\zeta_j^t,t)dz$$
$$-\frac{\pi^2\epsilon D_{min}}{4p_j^2}\int_{\tilde z_j}^{\tilde z_{j+1}}e^T(\tilde\zeta_j^t,t)e(\tilde\zeta_j^t,t)dz \tag{65}$$

Table 1
Parameter values.

Parameters	Numerical values
l	1 m
k_A	18.1 (h weight fraction)$^{-1}$
k_B	1.7 h^{-1}
k_C	4.8 (h weight fraction)$^{-1}$
d	0.5 m^{2}h^{-1}
υ	2 mh^{-1}
$x_{A,in}$	0.7 weight fraction
$x_{B,in}$	0 weight fraction

where

$$p_j^2 = \max\{(\zeta_j+\varepsilon_j-\tilde{z}_j)^2, (\tilde{z}_{j+1}-\zeta_j+\varepsilon_j)^2\},$$

for all $j \in \mathbb{N}_{n_y}$.

Hence, the inequality in (54) holds by taking into account (65) with the substitution of $e(\zeta_j, t)$ by $e(\tilde{\zeta}_j^t, t)$). Finally, conditions (55) and (57) ensure that

$$\|e(\cdot, t)\| \le M_e(e_0)\mathrm{e}^{-\gamma t}$$

holds for all $t \ge 0$, with $M_e(e_0)$ as defined in (37). □

Remark 2. An analytical feasibility analysis of the conditions in Theorems 1 and 2 is burdensome. By evaluating the solution of LMIs (44) and (45), it can be easily shown that the assumption $d_i \ge D_{\min} > 0$ is a necessary condition to find a solution for (44) and (45). A more detailed feasibility analysis is quite intricate. Nevertheless, a numerical analysis via feasibility regions may provide a good view of the method applicability under different numerical values of system and design parameters as achieved in Section 5.

5. Application example

As a case study, a tubular catalytic cracking reactor is considered. Indeed, catalytic cracking is one of the most important conversion processes in petroleum refineries. It is widely used to convert high-boiling, high-molecular weight hydrocarbon fractions of petroleum crude oils into more valuable gasoline, olefinic gases and other products [28]. Particularly, a tubular catalytic cracking reactor is considered where the following reactions occur

$$\begin{aligned} &A \overset{k_A}{\rightarrow} B \overset{k_B}{\rightarrow} C, \\ &A \overset{k_C}{\rightarrow} C, \end{aligned} \tag{66}$$

where A represents gas oil, B gasoline and C other products (e.g butanes, coke, etc.) and x_A and x_B the weight fractions of reactants A and B, respectively. Considering an isothermal process with axial dispersion, mass balances within the reactor yield the following parabolic PDE system [28]

$$\begin{aligned} \partial_t x_A(z,t) &= d\partial_z^2 x_A(z,t) - \upsilon \partial_z x_A(z,t) \\ &\quad - (k_A + k_C)x_A^2(z,t), \\ \partial_t x_B(z,t) &= d\partial_z^2 x_B(z,t) - \upsilon \partial_z x_B(z,t) \\ &\quad + k_A x_A^2(z,t) - k_B x_B(z,t), \end{aligned} \tag{67}$$

along with the boundary conditions

$$\begin{aligned} &d\partial_z x_A(0,t) = \upsilon(x_A(0,t) - u_A(t)), \\ &d\partial_z x_B(0,t) = \upsilon(x_B(0,t) - u_B(t)), \\ &\partial_z x_A(l,t) = 0, \\ &\partial_z x_B(l,t) = 0. \end{aligned} \tag{68}$$

In the above equations, k_A, k_B and k_C are the kinetic constants of the reactions; d, υ, $x_{A,in}$ and $x_{B,in}$ are the axial dispersion coefficient, the superficial velocity, the inlet weight fraction of component A and the inlet weight fraction of component B, respectively.

Table 2
$\gamma_{\max}$ of the proposed approach for different combinations of m and q.

(m, q)	$\gamma_{\max}$
(3, 2)	1.2
(4, 2)	3.4
(5, 2)	4.5

The adopted numerical values for the process parameters are taken from Table 1.

The system modeled by (67)–(68) takes the form of (6)–(7) by considering

$$\begin{aligned} &x(z,t) = \begin{bmatrix} x_A(z,t) & x_B(z,t) \end{bmatrix}^T, \; u_d = 0, \\ &u_0(t) = \begin{bmatrix} x_{A,in} & x_{B,in} \end{bmatrix}^T, \; u_1(t) = 0, \\ &D = d\,I, \; \mathcal{V} = \upsilon\,I, \; K = \mathrm{diag}(0, k_B), \\ &B = 0, \quad G = \begin{bmatrix} -(k_A + k_C) \\ k_A \end{bmatrix}, \\ &M_{\alpha_0} = \frac{d}{\upsilon} I, \; M_{\beta_0} = -I, \; M_{\alpha_1} = I, \; M_{\beta_1} = 0, \\ &r(x) = x_A^2. \end{aligned} \tag{69}$$

with rate function defined as $r(x) = x_A^2$ and corresponding Jacobian given by $\nabla_x r(x) = \begin{bmatrix} 2x_A & 0 \end{bmatrix}$. Considering the domain of operation of the state variables

$$\mathfrak{D} = \left\{(x_A, x_B) \in \mathbb{R}^2 : 0 \le x_A \le 0.85\right\},$$

the local lower and upper bound matrices of the Jacobian matrix are respectively

$$\varGamma_1 = \begin{bmatrix} 0 & 0 \end{bmatrix} \qquad \varGamma_2 = \begin{bmatrix} 1.7 & 0 \end{bmatrix}. \tag{70}$$

The online measurement vector is given by one piecewise measurement

$$y(t) = \frac{1}{2\varepsilon_1} \int_{\zeta_1 - \varepsilon_1}^{\zeta_1 + \varepsilon_1} x_A(z,t) dz, \tag{71}$$

which sets $\mathbf{c}_1(z) = \frac{1}{2\varepsilon_1} 1_{[\zeta_1-\varepsilon_1, \zeta_1+\varepsilon_1]}$, $c_1 = [1 \; 0]^T$. To obtain the output injection gain $L_D : [0, 1] \to \mathbb{R}^{2\times 1}$ through the application of Theorem 2 we assume that $\zeta_1 = 0.75$ and $\varepsilon_1 = 0.01$. Thus, we solve the LMI in (44) for different values of m and q and using bisection search we calculate $\gamma_{\max}$ for each case. The results are given in Table 2.

5.1. Observer tests

The observer and system responses are generated via numerical simulation with initial profiles $x_A(z,0)$, $x_B(z,0)$, $\hat{x}_A(z,0)$ and $\hat{x}_B(z,0)$ in the form of positive polynomials satisfying the boundary conditions and matching the initial output measurement so as to obtain a faster convergence. Figs. 6 and 7 show the evolution of the actual profiles of x_A and x_B (red lines) with their respective estimation $\hat{x}_A$ and $\hat{x}_B$ (blue lines) in four different time instants.

Fig. 8 shows the evolution of the estimation error norm. Since the generated initial estimation profiles are already a good approximation of the actual state variables, the estimation error norm converges quickly, and hence, provides very satisfactory estimates.

The semi-definite programming framework for the observer synthesis allows assessing the feasibility of the method under different numerical values of system and design parameters. Namely, the dependence among the design and system parameters can be analyzed by solving the LMIs related to Theorems 1 and 2 for different parameter values. This numerical feasibility

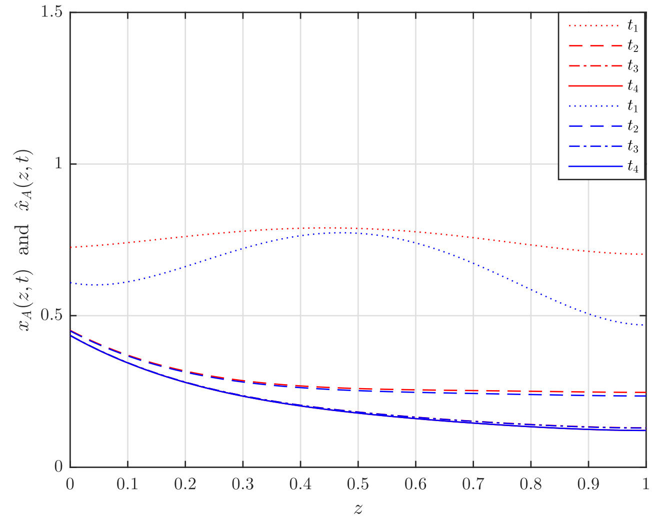

Fig. 6. Time evolution of the spatial profile of $x_A(z,t)$ and $\hat{x}_A(z,t)$ at time instants $t_1 = 0$, $t_2 = 0.12$, $t_3 = 0.36$, $t_4 = 0.6$.

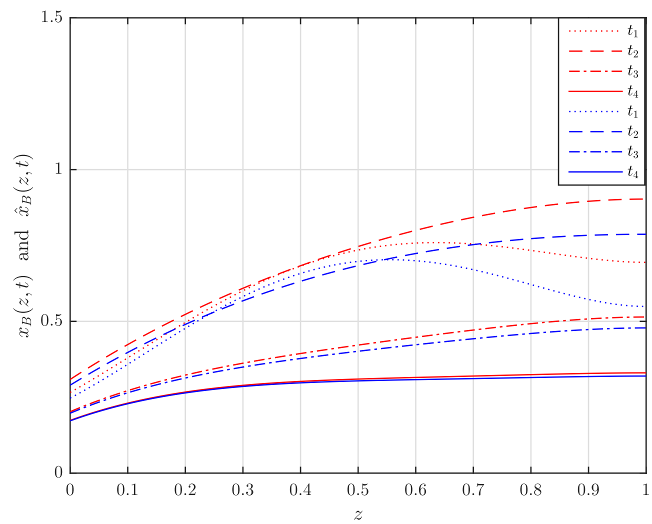

Fig. 7. Time evolution of the spatial profile of $x_B(z,t)$ and $\hat{x}_B(z,t)$ at time instants $t_1 = 0$, $t_2 = 0.12$, $t_3 = 0.36$, $t_4 = 0.6$.

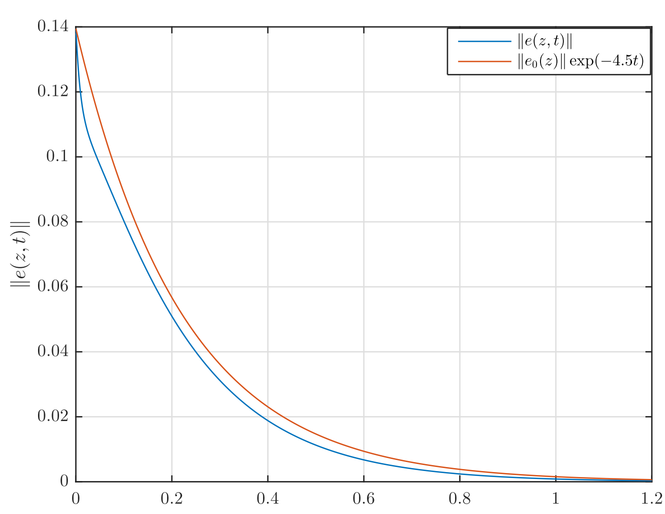

Fig. 8. Time evolution of the estimation error norm $\|e(z,t)\|$.

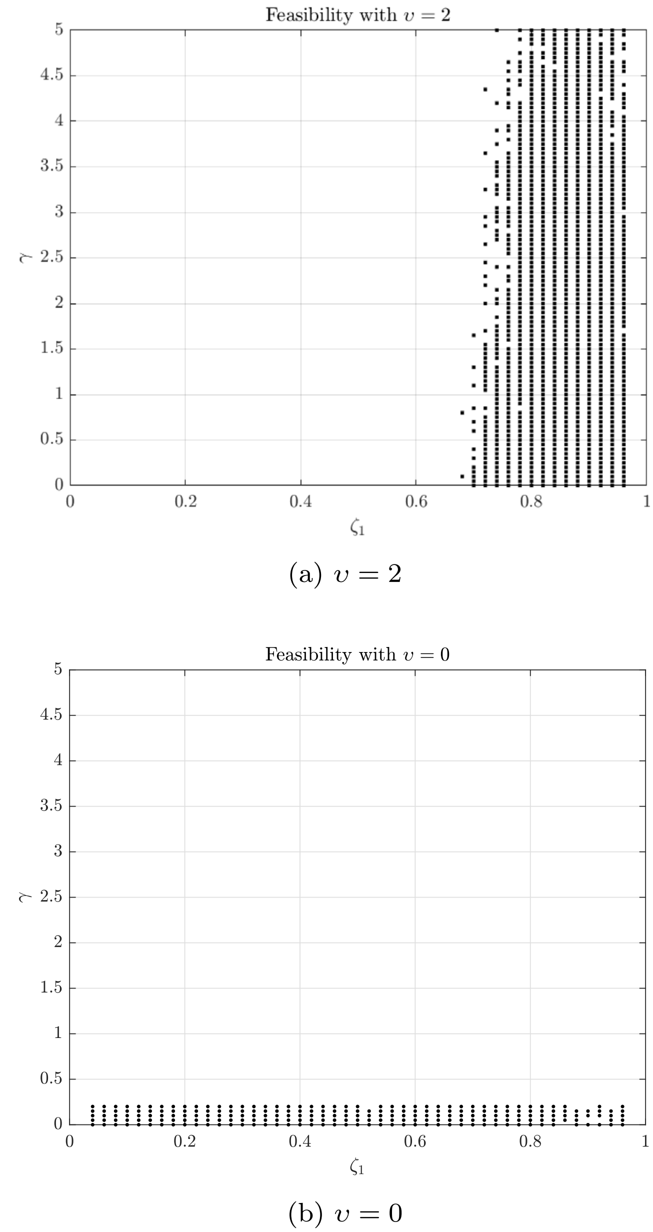

Fig. 9. Feasibility regions related to superficial velocity υ.

analysis may be used to determine the location of the unique available sensor as well as to analyze the sensitivity with respect to model parameters in our example. In this context, Fig. 9 shows the feasibility region of the LMIs conditions (44) and (45) with respect to the sensor position ζ_1 and the lower bound of the decay rate γ keeping the same numerical values for the other design parameters.

As it may be seen in Fig. 9, the proposed methodology finds feasible solutions even when the superficial velocity υ is set to zero. These results are logical from a physical point of view since a zero velocity (subfigure b) corresponds to a purely diffusive system where the information travels equally in all directions and where indeed the position of the sensor is indifferent, whereas a more convective system (subfigure a) implies a position of the sensor towards the end of the reactor. It is well known that a purely convective system would imply the use of a sensor located at the reactor outlet. For convective–diffusive systems, a local optimum sensor location can be determined in order to improve the convergence of the estimation error which is defined by the numerical value of γ.

6. Conclusion

In this work, a late lumping approach is proposed for the observer design of transport-reaction systems described by a set of coupled semilinear parabolic PDEs. In particular, the Lyapunov theory is applied to derive observer design conditions in terms of LMI constraints considering a Lure type representation of the estimation error dynamics and a sector condition obtained from a boundedness assumption on Jacobian matrices, which reduces the conservatism of the treatment of the nonlinearity of the model in comparison with the only use of the local Lipschitz constant to derive the corresponding LMI constraints. In contrast, some inevitable degree of conservatism is added by the inclusion of the auxiliary variables $\{\tilde{z}_j : j \in \mathbb{N}_{n_y+1}\}$ which may modify the feasible solutions according to their numerical selection. The proposed methodology is also based on a polynomial parametrization of the Lyapunov functional candidate and observer gain which is verified by means of standard semi-definite programming tools that also allow performing a numerical feasibility analysis to assess the method applicability under different numerical values of system and design parameters as achieved in Section 5 for the nonisothermal tubular reactor model. These numerical simulations demonstrate the observer performance in realistic scenarios.

CRediT authorship contribution statement

Ivan F.Y. Tello: Conceptualization, Methodology, Software, Writing – original draft, Visualization, Investigation, Software, Validation, Writing – review & editing. **Alain Vande Wouwer:** Conceptualization, Methodology, Visualization, Investigation, Supervision, Writing – review & editing. **Daniel Coutinho:** Conceptualization, Methodology, Visualization, Investigation, Supervision, Writing – review & editing.

Declaration of competing interest

The authors declare that they have no known competing financial interests or personal relationships that could have appeared to influence the work reported in this paper.

Appendix

Consider first the one-dimensional integral

$$\int_a^b e^T(z)\tilde{\mathcal{V}}(z)\partial_z e(z)dz = \sum_{i,j}^{n}\int_a^b e_i(z)\tilde{v}_{ij}(z)\partial_z e_j(z)dz \tag{72}$$

with $\tilde{\mathcal{V}} : [a,b] \to \mathbb{R}^{n_x \times n_x}$ and $\tilde{v}_{ij}(z)$ being the (i,j) entry of $\tilde{\mathcal{V}}(z)$. Thus, integrating by parts the terms of the summation, it is easy to show that

$$\int_a^b e^T(z)\left(\tilde{\mathcal{V}}(z) + \tilde{\mathcal{V}}^T(z)\right)\partial_z e(z)dz = e^T(z)\tilde{\mathcal{V}}(z)e(z)\Big|_a^b - \int_a^b e^T(z)\partial_z\tilde{\mathcal{V}}(z)e(z)dz. \tag{73}$$

If $\mathcal{V} : [a,b] \to \mathbb{S}^{n_x}$, then we have

$$\int_a^b e^T(z)\tilde{\mathcal{V}}(z)\partial_z e(z)dz = \frac{1}{2}e^T(z)\tilde{\mathcal{V}}(z)e(z)\Big|_a^b - \frac{1}{2}\int_a^b e^T(z)\partial_z\tilde{\mathcal{V}}(z)e(z)dz. \tag{74}$$

Similarly, considering the integral

$$\int_a^b e^T(z)\tilde{D}(z)\partial_z^2 e(z)dz = \sum_{i,j}^{n}\int_a^b e_i(z)\tilde{d}_{ij}(z)\partial_z^2 e_j(z)dz. \tag{75}$$

with $\tilde{D} : [a,b] \to \mathbb{R}^{n_x}$. Thus, its integration by parts yields

$$\int_a^b e^T(z)\tilde{D}(z)\partial_z^2 e(z)dz = e^T(z)\tilde{D}(z)\partial_z e(z)\Big|_a^b - \int_a^b \partial_z e^T(z)\tilde{D}(z)\partial_z e(z)dz - \int_a^b e^T(z)\partial_z\tilde{D}(z)\partial_z e(z)dz. \tag{76}$$

If $\tilde{D} : [a,b] \to \mathbb{S}^{n_x}$, we can apply the identity in (74) into the last term of the right side of (76), thus we obtain

$$\int_a^b e^T(z)\tilde{D}(z)\partial_z^2 e(z)dz = e^T(z)\tilde{D}(z)\partial_z e(z)\Big|_a^b - \frac{1}{2}e^T(z)\partial_z\tilde{D}(z)e(z)\Big|_a^b + \frac{1}{2}\int_a^b e^T(z)\partial_z^2\tilde{D}(z)e(z)dz - \int_a^b \partial_z e^T(z)\tilde{D}(z)\partial_z e(z)dz. \tag{77}$$

References

[1] P.D. Christofides, J. Chow, Nonlinear and robust control of PDE systems: Methods and applications to transport-reaction processes, Appl. Mech. Rev. 55 (2) (2002) B29–B30.

[2] J.J. Winkin, D. Dochain, P. Ligarius, Dynamical analysis of distributed parameter tubular reactors, Automatica 36 (3) (2000) 349–361.

[3] A. Elkadry, Transmission rate in partial differential equation in epidemic models, 2013.

[4] A. Vande Wouwer, M. Zeitz, State estimation in distributed parameter systems, in: Control Systems, Robotics and Automation–Volume XIV: Nonlinear, Distributed, and Time Delay Systems-III, EOLSS Publications, 2009, p. 92.

[5] R.F. Curtain, H. Zwart, An Introduction to Infinite-Dimensional Linear Systems Theory, Vol. 21, Springer Science & Business Media, 2012.

[6] A. Schaum, T. Meurer, J.A. Moreno, Dissipative observers for coupled diffusion–convection–reaction systems, Automatica 94 (2018) 307–314.

[7] A. Smyshlyaev, M. Krstic, Backstepping observers for a class of parabolic PDEs, Systems Control Lett. 54 (7) (2005) 613–625.

[8] A. Baccoli, A. Pisano, Anticollocated backstepping observer design for a class of coupled reaction-diffusion PDEs, J. Control Sci. Eng. 2015 (2015) 53.

[9] B.-N. Liu, D. Boutat, D.-Y. Liu, Backstepping observer-based output feedback control for a class of coupled parabolic PDEs with different diffusions, Systems Control Lett. 97 (2016) 61–69.

[10] Y.V. Orlov, Sliding mode observer-based synthesis of state derivative-free model reference adaptive control of distributed parameter systems, J. Dyn. Sys., Meas., Control 122 (4) (2000) 725–731.

[11] Y.V. Orlov, S. Chakrabarty, D. Zhao, S.K. Spurgeon, Sliding mode observer design for a parabolic PDE in the presence of unknown inputs, Asian J. Control 21 (1) (2019) 224–235.

[12] J.F. Sturm, Using SeDuMi 1.02, a MATLAB toolbox for optimization over symmetric cones, Optim. Methods Softw. 11 (1–4) (1999) 625–653.

[13] F. Castillo, E. Witrant, C. Prieur, L. Dugard, Boundary observers for linear and quasi-linear hyperbolic systems with application to flow control, Automatica 49 (11) (2013) 3180–3188.

[14] E. Fridman, Observers and initial state recovering for a wave equation: an LMI approach, IFAC Proc. Vol. 46 (3) (2013) 337–342.

[15] A. Schaum, J.A. Moreno, E. Fridman, J. Alvarez, Matrix inequality-based observer design for a class of distributed transport-reaction systems, Internat. J. Robust Nonlinear Control 24 (16) (2014) 2213–2230.

[16] J.-W. Wang, Y. Guo, Distributed-parameter Luenberger observer for semi-linear parabolic PDE systems with a mobile pointwise sensor, in: 2016 35th Chinese Control Conference, CCC, IEEE, 2016, pp. 1366–1371.

[17] A. Papachristodoulou, M.M. Peet, On the analysis of systems described by classes of partial differential equations, in: Proceedings of the 45th IEEE Conference on Decision and Control, IEEE, 2006, pp. 747–752.

[18] A. Gahlawat, M.M. Peet, A convex sum-of-squares approach to analysis, state feedback and output feedback control of parabolic PDEs, IEEE Trans. Automat. Control 62 (4) (2017) 1636–1651.
[19] A. Gahlawat, M.M. Peet, Optimal state feedback boundary control of parabolic PDEs using SOS polynomials, in: 2016 American Control Conference, ACC, IEEE, 2016, pp. 4350–4355.
[20] A. Papachristodoulou, J. Anderson, G. Valmorbida, S. Prajna, P. Seiler, P.A. Parrilo, Sum of Squares Optimization Toolbox for MATLAB User's Guide, University of Oxford, 2013.
[21] E. Fridman, Y.V. Orlov, An LMI approach to H_∞ boundary control of semilinear parabolic and hyperbolic systems, Automatica 45 (9) (2009) 2060–2066.
[22] E. Fridman, Observers and initial state recovering for a class of hyperbolic systems via Lyapunov method, Automatica 49 (7) (2013) 2250–2260.
[23] E. Meyer, M.M. Peet, A convex approach for stability analysis of coupled PDEs using Lyapunov functionals, 2016, arXiv:1602.06986.
[24] A. Zemouche, M. Boutayeb, G.I. Bara, Observer design for nonlinear systems: An approach based on the differential mean value theorem., in: Proceedings of the 44th IEEE Conference on Decision and Control, IEEE, 2005, pp. 6353–6358.
[25] G.H. Hardy, J.E. Littlewood, G. Pólya, Inequalities, Cambridge University Press, Cambridge, 1952.
[26] B. Açıkmeşe, M. Corless, Observers for systems with nonlinearities satisfying incremental quadratic constraints, Automatica 47 (7) (2011) 1339–1348.
[27] S. Boyd, L. El Ghaoui, E. Feron, V. Balakrishnan, Linear Matrix Inequalities in System and Control Theory, SIAM, 1994.
[28] V.W. Weekman Jr., Kinetics and dynamics of catalytic cracking selectivity in fixed-bed reactors, Ind. Eng. Chem. Process Des. Dev. 8 (3) (1969) 385–391.